A Model for Heat-Affected Zone Hardness Profiles in Al-Li-X Alloys

A semi-empirical model is proposed to predict variation in HAZ hardness profiles in a new generation of alloys

BY G. O. RADING AND J. T. BERRY

ABSTRACT. A model based on reaction kinetics and elemental diffusion is proposed to account for the presence of double inflection in the hardness profiles of the heat-affected zone (HAZ) in weldments of Al-Li-X alloys tested without postweld heat treatment (PWHT). Such profiles are particularly evident when 1) the base metal is in the peak-aged (T8 or T6) temper condition prior to welding; 2) the welding process is a high-heat input process, *i.e.*, gas tungsten arc (GTA), gas metal arc (GMA) or plasma arc (PA) welding; and 3) a filler alloy deficient in lithium (*i.e.*, AA 2319) is used. In the first part of this paper, the theoretical mechanisms are presented. It is proposed that the double inflection appears due to complete or partial reversion of the semi-coherent, plate-like precipitates (*i.e.*, θ′, T_1 or S′); coarsening of the plate-like precipitates at constant volume fraction; precipitation of δ′ as a result of natural aging; and diffusion of lithium from the HAZ into the weld pool due to the concentration gradient between the weld pool and the base metal. In the second part (to be published in next month's *Welding Journal*), experimental validation of the model is provided using weldments of the Al-Li-Cu Alloy 2095.

Introduction

Hardness profiles in the heat-affected zones (HAZ) of the new generation Al-Li-X alloys (where X is usually copper or magnesium) generally show double inflection if the weldments are tested without postweld heat treatment (PWHT). This is particularly notable under the following conditions:

- The base metal (BM) is in the peak aged (T8 or T6) temper condition prior to welding.
- The welding is carried out using a high-heat input process such as gas tungsten arc (GTA), gas metal arc (GMA) or plasma arc (PA) welding.
- The filler alloy used is deficient in lithium. Aluminum Alloy 2319 is the most often used filler alloy (Ref. 1).

On the contrary, HAZ hardness profiles in similar weldments made by the low-heat input processes such as electron beam (EB) or laser beam (LB) (Ref. 2) and autogenous welds (Ref. 3) generally show a monotonic increase in hardness from the weld metal (WM) to the base metal. Examples of HAZ hardness profiles showing double inflection can be seen in the work of Biermann, *et al.* (Ref. 4), on AA 2091; Cross, *et al.* (Ref. 2), on AA 2095; Zacharia, *et al.* (Ref. 5), on AA 2090; and Fridlyander, *et al.* (Ref. 6), on Soviet Alloy 1460, among others. Two of these results are reproduced in Fig. 1. One notable departure from this trend is in the work of Martukanitz, *et al.* (Ref. 7), on AA 2090, where a monotonic increase in hardness is reported.

KEY WORDS

AL-Li-x Alloys
Base metal (BM)
Diffusion
Heat-Affected Zone (HAZ)
Inflection
Postweld Heat Treatment
Precipitate
Weld interface

The reasons for the occurrence of double inflection have not been explored despite the importance of this phenomenon to the overall weldment strength and to any PWHT procedures that may be adopted to improve the weldment strength. In the first part of the current study, a theoretical model based on reaction kinetics during welding (dissolution and coarsening of one type of precipitate and reprecipitation of a less potent one due to natural aging) and elemental diffusion due to differences in chemistry between the BM and filler alloy is developed. In the second part, experimental evidence is provided to validate the model.

The Model

Introduction

The weld thermal cycle induces changes in the HAZ microstructure due to precipitate dissolution, reprecipitation and coarsening. The exact nature and extent of these changes varies from point to point in the HAZ, depending on the thermal experience (which depends on the distance of the point in question from the weld pool). These microstructural changes induce variations in the strength/hardness of the HAZ. The total hardness at a point in the HAZ may be written as a sum from several hardening mechanisms:

$$H = H_i + H_{ss} + H_{gb} + H_t + H_d + H_p \quad (1$$

where subscripts refer to the contribution to hardness due to intrinsic hardness of the aluminum, solution hardening, grain boundary hardening (Hall-Petch effect), texture, dislocations (work hardening) and precipitation hardening, respectively. When there are several precipitates contributing to the hardening, the term H_p may be broken down into several components:

G. O. RADING is with the Department of Engineering Science and Mechanics, University of Alabama, Tuscaloosa, Ala., and J. T. BERRY is with the Department of Metallurgical and Materials Engineering, University of Alabama, Tuscaloosa, Ala.

$$H_p = H_{p1} + H_{p2} + \kappa + H_{pn} \qquad (2)$$

Equation 2 applies if it is assumed that the contributions from the different precipitates are linearly additive.

Assumptions

In developing the model, the following assumptions were made:

1) The BM is in peak-aged condition prior to welding and precipitation hardening is provided by one precipitate only. The precipitate is one of the plate-like precipitates that may form in Al-Li-X alloys (*i.e.*, T_1 [Al_2CuLi], θ′[Al_2Cu] or S′ [Al_2MgCu]).

2) Hardness changes in the HAZ result only from changes in precipitation. This is not strictly correct because the thermal experience has an effect on the grain size, solution strengthening (*i.e.*, dissolution of precipitates results in an increase in the solute content), dislocation structure and possibly the texture. However, for a peak-aged alloy the assumption is reasonable, because precipitate hardening predominates.

3) Incoherent grain boundary precipitates have no effect on the hardness.

4) Only one type of precipitate forms (as a result of natural aging) after dissolution of the first precipitate (in this case, δ′).

5) The theory applies only to a single-pass weld.

6) The thermal properties of the material are independent of temperature.

7) The material welded is a thin plate; hence, thickness variations in temperature are negligible.

8) Latent heat losses are negligible. This assumption is reasonable since heat expended in melting is regained when the weld solidifies.

9) Heat losses from the surface of the plate are negligible. This, together with assumption 7 above and a high welding speed (compared to the thermal diffusivity of the material), reduces the problem to a one-dimensional heat flow problem.

The Concept

During welding, the HAZ is subjected to a thermal cycle. The peak temperature, T_p, of this thermal cycle varies with the distance y from the weld interface (WI) and has a maximum at the WI and a minimum, T_o, (equal to the room or preheat temperature) in the far unaffected BM. This thermal cycle leads to several effects with the principal ones as follows:

1) Dissolution (reversion) and coarsening (overaging) of the plate-like strengthening Precipitate (T_1, θ′ or S′), referred to as *precipitate* 1 (P1). Starting from the portion of the HAZ closest to the unaffected BM, the precipitate partially dissolves and the solutes remain in solution in the matrix. This results in reduction of the volume fraction of P1. Closer to the WI (where a higher peak temperature is attained), the partial dissolution of P1 is followed by coarsening (overaging) while maintaining an almost constant volume fraction. The boundary between the two regions (*i.e.*, the region of pure dissolution and that of dissolution accompanied by coarsening) will be designated y_{c3}. The severity of the coarsening increases as the WI is approached. Still closer to the WI, the overaged precipitates start dissolving, thus producing a supersaturated matrix. In the region just adjacent to the WI, the dissolution of P1 is complete. This region may be referred to as the fully-reverted region, in which P1 makes no contribution to precipitation hardening. In the rest of the HAZ, the contribution of P1 to precipitation hardening, ΔH_{p1}, increases with the distance from the WI, y. If precipitate dissolution was the only mechanism responsible for HAZ softening, the variation of HAZ hardness with y would be as shown in Curve 1 of Fig. 2, where $H = H_o$ (H_o = contribution to the hardening by all other mechanisms except precipitation) up to the boundary of the fully-reverted region y_{c1}, rising to $H = H_{max}$ at the maximum extent of the HAZ ($y = y_{max}$). Here, H_{max} is the original BM hardness. Hence, the hardness profile can be written as:

$$\begin{aligned} H &= H_o & 0 < y < y_{c1} \\ H &= H_o + \Delta H_{p1} & y_{c1} < y < y_{max} \\ H &= H_{max} & y > y_{max} \end{aligned} \qquad (3)$$

2) Natural aging. When the supersaturated solution formed from P1 cools to room temperature, a natural aging phenomenon occurs through precipitation of δ′ (Al_3Li), which will be termed Precipitate 2 (P2). The resulting hardness increase due to P2 will be designated ΔH_{p2}. Consequently, the resulting hardness should be constant in the fully-reverted region and should then fall off to H_o at the distance y_{c2}, from the WI. The reason is that increasingly less solute is available for natural aging as we move away from the WI. Therefore, if this was the only operating mechanism, then

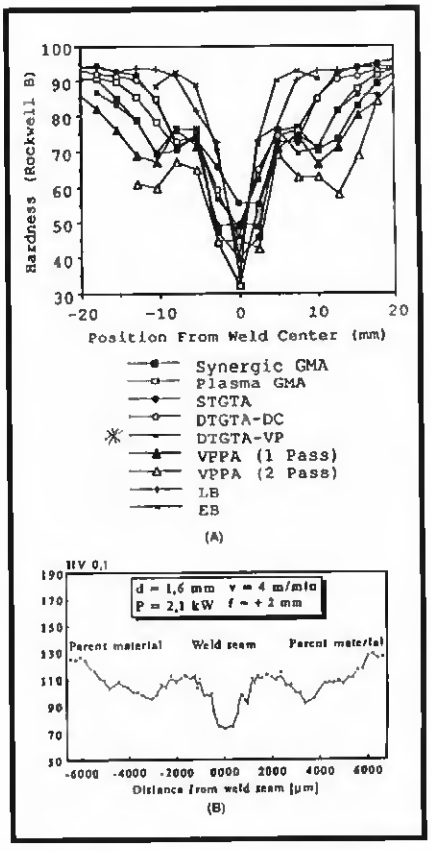

Fig. 1 — Examples of HAZ hardness profiles in Al-Li-X alloys. A — AA 2095 (Ref. 2); B — AA 2091 (Ref. 4).

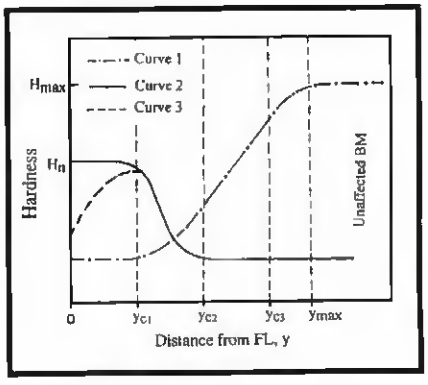

Fig. 2 — Schematic variation of HAZ hardness with distance from fusion line FL (Curve 1 — precipitate dissolution and coarsening; Curve 2 — natural aging; Curve 3 — back diffusion).

$$\begin{aligned} H &= H_o + \Delta H_n & 0 < y < y_{c1} \\ H &= H_o + \Delta H_{p2} & y_{c1} < y < y_{c2} \\ H &= H_o & y > y_{c2} \end{aligned} \qquad (4)$$

where ΔH_n is the maximum possible increase in hardness due to P2. This variation is shown schematically as Curve 2 in Fig. 2.

3) Elemental diffusion. If the weld pool (filler metal) is deficient in lithium, diffusion into the weld pool will take place. The extent of lithium depletion will be highest close to the WI due to the higher temperature attained and the shorter diffusion distances involved. Since lithium is necessary for the formation of δ' (and, hence, for postweld natural aging), the effect of natural aging will be lower close to the WI. It can be reasonably assumed that diffusion is pronounced only in the fully-reverted region ($y < y_{c1}$) because this region already has the maximum possible amount of lithium in solution, attains the highest temperature and is closest to the weld pool. Therefore, the net hardness in the fully reverted region can be estimated by substitution into Equation 4, except that ΔH_{p2} must be determined after taking lithium diffusion into account. This varition is shown schematically as Curve 3 in Fig. 2.

As shown in Fig. 3, the HAZ can be divided into four distinct regions in which the different mechanisms (*i.e.*, dissolution, overaging, diffusion and natural aging) dominate.

Region I — The fully-reverted region. P1 is fully dissolved and natural aging would have reached its maximum potential, but this is affected by diffusion of lithium into the weld metal. Precipitation hardening is provided only by δ' and, therefore, the net hardness rises to a maximum in the vicinity of y_{c1}.

Region II — The partially aged region. In this region, some P1 has dissolved into the matrix and the dissolved solutes contribute to natural aging after the weldment has cooled. The undissolved P1 has overaged. Precipitation hardening results from contributions of both natural aging (δ') and the overaged P1. The second point of inflection occurs in this region at the point where Curve 1 and Curve 2 intersect — Fig. 2.

Region III — The overaged region. In this region, there is no contribution from natural aging. Precipitation hardening is provided only by the overaged P1.

Region IV — The partially reverted region. In this region, the decrease in hardness (compared to the BM) results only from the decrease in the volume fraction of P1 as a result of partial dissolution. A similar argument has been advanced by Myhr and Grong (Ref. 8). However, their model does not consider back diffusion, which was not an important factor in the alloy/filler system they considered, or precipitate coarsening. Mathematical relations are now proposed for ΔH_{p1} and ΔH_{p2} in each of the four regions. Since these depend on the thermal cycle, this is considered first.

HAZ Thermal Cycle

The temperature profile in the HAZ can be calculated from the Rosenthal equation as reformulated by Easterling (Ref. 9). Considering the welding torch as a point source moving with constant velocity, v, the heat flux, q, is given by

$$q = \eta VI \tag{5}$$

where η is the arc efficiency, V is the welding voltage and I is the welding current. Considering the case of a thin plate of thickness, d, the problem reduces to a one-dimensional heat flow problem and the following time-temperature variation is obtained (Ref. 9):

$$T = T_o \frac{\eta VI / vd}{\rho c\sqrt{(4\pi\alpha t)}} \exp\left(-r^2 / 4\alpha t\right) \tag{6}$$

where α is the thermal diffusivity, ρ is the density, c is the specific heat capacity of the material being welded and T_o is as defined earlier. For a one-dimensional problem, $r = y$, the distance from the weld centerline. Thus, at any point in the HAZ, the time-temperature distribution is as shown in Fig. 4. If T_p is the peak temperature at point y, then by differentiating Equation 6 and setting to zero (at peak temperature, $dT/dt = 0$),

$$T_p - T_o = \sqrt{(2/\pi e)} \frac{\eta VI}{vd\rho c 2y}. \tag{7}$$

The time to reach peak temperature, τ, is the time constant for the position of the HAZ and can be found by substituting for T_p from Equation 7 into Equation 6:

$$\tau = \frac{(\eta VI / vd)^2}{4\pi e\lambda\rho c\left(T_p - T_o\right)^2} \tag{8}$$

where λ is the thermal conductivity.

Precipitate Dissolution Kinetics

The changes taking place in the HAZ occur under non-isothermal conditions. Hence, both temperature and time have to be considered in determining the kinetics of reactions. In this work, the approach to non-isothermal kinetics adopted by Ion, Easterling and Ashby (Ref. 10), Ashby and Easterling (Ref. 11) and Myhr and Grong (Ref. 8) will be adopted (*i.e.*, a "kinetic strength" of the thermal cycle defined below will be evaluated). If the volume fraction of the precipitate at any time τ, is f_1, dissolution is diffusion controlled. Then,

$$\frac{df_1}{dt} = k_1 f(f_1) \exp\left[-Q_d / RT(t)\right] \tag{9}$$

where Q_d is the activation energy for dissolution, $f(f_1)$ is some function of f_1, k_1 is a kinetic constant and R is the gas constant. Then, the kinetic strength of the thermal cycle, I, is defined as the total change in f_1 during the cycle:

$$I = \int_0^\infty k_1 \exp\left[-Q_d / RT(t)\right] dt. \tag{10}$$

Ratio β can then be defined as

$$\beta = \frac{\int_0^\infty \exp\left[-Q_d / RT(t)\right] dt}{\tau \exp\left(-Q_d / RT_p\right)}. \tag{11}$$

Ion, *et al.* (Ref. 10), have shown that β can be approximated by

$$\beta = 2\left\{\pi RT_p / Q_d\right\}^{1/2} \tag{12}$$

and I then becomes:

$$I = \beta\tau \exp\left(-Q_d / RT_p\right) \tag{13}$$

The volume fraction of the matrix available for dissolution, f, in the non-isothermal cycle can then be calculated from (Ref. 10):

$$f = 1 - \exp\left\{-\frac{\beta\tau}{\beta^*\tau^*} - \frac{Q_2}{R}\left[\frac{1}{T_p} - \frac{1}{T^*}\right]\right\}^{3/2} \tag{14}$$

where τ^* is the time constant required for complete dissolution of P1 at temperature, T^*, and Q_2 is the activation energy for diffusion of the slowest diffusing element in P1. Then, f_1 can be calculated from $f_1 = 1 - f$.

Constitutive Equations

The relation between the volume fraction of P1 and its contribution to precipitate hardening can be determined from first principles or taken from the literature. For example, if P1 is T_1, Huang and Ardell (Ref. 12) have proposed that

$$\Delta\tau_{T1} = \frac{Gb}{2\pi\sqrt{(1-\nu)}} \sqrt{\left(f_{T1} / 2rB\right)} \frac{\ln(2r/\pi b)}{1.43 - f_{T1}^{1/2}} \tag{15}$$

where f_{T1} is the volume fraction of T_1, β is the associated thickness, G is the shear modulus, b is Burger's vector and ν is Poisson's ratio. $\Delta\tau_{T1}$ is proportional to ΔH_{T1}, and, hence, ΔH_{p1} can be expressed as

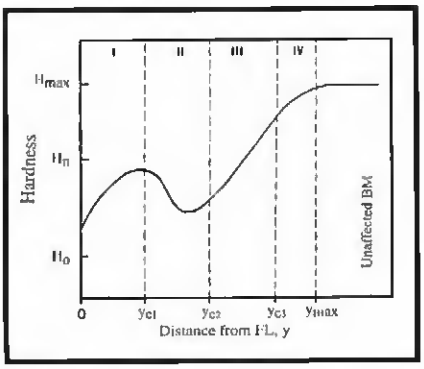

Fig. 3 — Net HAZ hardness profile showing distinct regions. (Region I — fully reverted region; Region II — partially aged region; Region III — overaged region; Region IV — partially reverted region.)

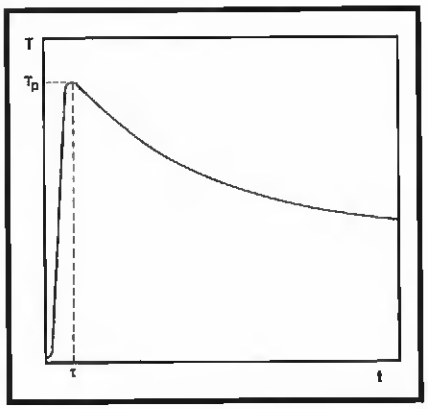

Fig. 4 — Typical thermal cycle at a point in the HAZ (schematic).

$$\Delta H_{p1} = C_1\left[f_{p1}\right]^{1/2} \tag{16}$$

where C_1 is a constant. This is the expression for ΔH_{p1} in Region IV where dissolution of P1 without subsequent coarsening is the dominant mechanism. Since it is assumed that no coarsening takes place during this phase of dissolution, no change in hardening results from a change in precipitate size (*i.e.*, r and B are taken as constant).

Natural Aging

The natural aging is assumed to take place following the dissolution of P1. The new precipitate, P2, must be able to form without formal solution treatment and quenching. Furthermore, P2 can form only where dissolution has taken place since it is assumed that elements dissolved from P1 participate in the formation of P2. In Al-Li-X alloys, all these conditions are met by δ′, since numerous studies have confirmed δ′ forms without solution treatment in these alloys (Refs. 13, 14). This precipitation can be assumed to be an isothermal reaction taking place at room temperature after the weldment has cooled. In the fully-reverted region, all the solute that can be dissolved is in solution, and, therefore, the maximum hardness attainahle from P2 (with this amount of solute) is proportional to the amount of P1 dissolved. Again, the relation between this volume fraction and contribution to precipitate hardening can he derived from first principles. However, for Al-Li-X alloys, P2 is δ′; hence, a constitutive equation for hardening due to natural aging can be estimated from Huang and Ardell (Ref. 15) (assuming an underaged condition) as follows:

$$\Delta\tau_{\delta'} = \frac{\gamma_{apb}}{2b}\left[\frac{3\pi^2\gamma_{apb}f_{\delta'}(r)}{32\Gamma}\right] \tag{17}$$

where $f_{\delta'}(r)$ is the volume fraction of δ′ as a function of the radius of the precipitate, r, Γ is the line tension on a dislocation shearing through the precipitates and γ_{apb} is the antiphase boundary energy. Assuming again that $\Delta\tau$ is proportional to ΔH, a first approximation relation for ΔH_{p2} can be written as

$$\Delta H_{p2} = C_2\left(f_{\delta'}\right)^{1/2} \tag{18}$$

where C_2 is another constant. Here again, the effect of change in particle radius is neglected. From the assumptions made earlier, $\Delta H_{p2} = 0$ for $y > y_{c2}$.

Elemental Diffusion

In Al-Li-X alloy weldments, lithium diffusion to the weld pool will take place if a lithium-deficient filler alloy is used. This is due not only to the concentration gradient but also to the highly-diffusive nature of lithium in aluminum. As a consequence, the amount of lithium available for formation of δ′ is reduced. The concentration profile may be estimated from Fick's second law:

$$\frac{c(y)-C_w}{c_s-c_w} = \frac{1}{2}\left[1-erf\frac{-y}{2\sqrt{Dt}}\right] \tag{19}$$

where *erf* is the error function, D is the diffusivity of lithium in aluminum; c_s, $c(y)$ and c_w are the concentrations of lithium in the unaffected BM, at a distance, y, from the weld interface and in the WM, respectively. For a more realistic analysis, the following factors should also be taken into account:

1) The non-isothermal nature of the process.

2) The dependence of the diffusivity, D, on temperature.

3) The continuous variation of c_w with time.

4) The change of state of the WM from liquid to solid during the process.

5) The non-uniformity of c_w after weld solidification due to solute segregation. However, to a first approximation, c_w can be estimated from weld dilution.

For spherical precipitates, the volume fraction is proportional to the concentration squared (Ref. 8). Therefore, within the fully-reverted region

$$f_{\delta'} = f_{\delta'c1}\left[c(y)/c_{yc1}\right]^2 \tag{20}$$

where $f_{\delta'c1}$ and c_{yc1} are the volume fraction and lithium concentration at $y = y_{c1}$, respectively. ΔH_{p2} can then be estimated by suhstituting for $f_{\delta'}$ into Equation 18.

Precipitate Coarsening

The increase in the radius of P1 can be estimated from the Lifshitz-Slyozer-Wagner (LSW) coarsening theory, which, for a weld cycle with parameters τ and T_p, (defined earlier) can be written as (Ref. 10)

$$\frac{r^3-r_0^3}{r^*-r_0^3} = \frac{\alpha\tau T_p^*}{\alpha^*\tau^* T_p}\exp\left[Q/R\left(1/T_p^*-1/T_p\right)\right] \tag{21}$$

where r is the radius after aging at the peak temperature T_p for a period of time (represented by τ), r_o is the original radius, r^* is a known radius obtained after overaging at a known temperature T_p^* and time τ^*. The decrease in hardness due to overaging, ΔH_a, can then be estimated using the constitutive equation for the precipitate concerned:

$$\Delta H_a = g(r) \tag{22}$$

where $g(r)$ is some function of r. For example, in the case of T_1, Equation 15 can be rewritten as (assuming coarsening at constant volume fraction)

$$\Delta H_{aT1} = C_4\Delta\tau_{T1} = C_5\left[\ln r_0/\sqrt{r_o} - \ln r/\sqrt{r}\right] \tag{23}$$

where C_4 and C_5 are constants. Then,

$$\Delta H_{p1} = H_{\max} - H_o - \Delta H_a \tag{24}$$

Equation 24 is used to determine ΔH_{p1} in Regions II and III, where overaging is the mechanism that controls the contribution of P1 to the hardness.

Net Hardness

Assuming that the contributions of P1 and P2 to precipitation hardening are linearly additive, the resulting hardness profile through the HAZ can be summarized as follows:

$$
\begin{aligned}
H(y) &= H_o + \Delta H_{p2} && 0 < y < y_{c1} \\
&= H_{\max} + \Delta H_{p2} - \Delta H_a && y_{c1} < y < y_{c2} \\
&= H_{\max} - \Delta H_a && y_{c2} < y < y_{c3} \\
&= H_o + C_1 \left[f_{p1} \right]^{1/2} && y_{c3} < y < y_{\max} \\
&= H_{\max} && y > y_{\max}
\end{aligned}
\tag{25}
$$

where all the symbols have been defined previously and ΔH_{p2} for $0 < y < y_{c1}$ is calculated after taking lithium diffusion into consideration. The predicted hardness profile is shown in Fig. 3.

Predictive Capacity of the Model

In order to use the model to predict the hardness profile, it is necessary to know which precipitate (θ', T_1 or S') is the predominant strengthener in the BM prior to welding along with constitutive equations relating its volume fraction and radius to its contribution to strengthening (hardening). In addition, it is necessary to know its solvus temperature and the parameters T_p^*, t^*, r^*, Q_d and Q. For the specific material being welded, it also is necessary to have an estimate of r_o (the original mean radius of the precipitate) and its original volume fraction. Apart from T_p^*, t^* and r^*, the rest of the parameters are readily available in the literature. But, before the model can be used, it is necessary to show that the proposed microstructural evolution (*i.e.*, precipitate dissolution, coarsening) does take place. This is the object of part two of this paper (to be published next month).

Summary and Conclusion

A semi-empirical model is proposed to predict the variation of HAZ hardness profiles in weldments of the new generation Al-Li-X alloys, prepared in the peak-aged condition with a lithium-deficient filler alloy. Such profiles are predicted to show double inflection. It is suggested that this is due to the concurrent effects of dissolution and coarsening of the dominant plate-like precipitate (θ', T_1 or *S'*), natural aging due to precipitation of δ' after welding and diffusion of lithium from the HAZ into the weld pool. The first point of inflection (a maximum) corresponds to the point of maximum precipitation of δ', while the second point of inflection (a minimum) corresponds to the point where contribution of δ' and the overaged plate-like precipitate are equal. Equations are proposed to estimate the contribution of each effect (*i.e.*, dissolution, natural aging) to the hardness of the HAZ from the strength of the welding thermal cycle.

References

1. Srivastsan, T. S., and Sudarshan, T. S. 1991. Welding of lighweight aluminum-lithium alloys. *Welding Journal* 70(7): 173-s to 185-s.

2. Cross, C. E., Loechel, L. W., and Braun, G. F. 1992. *Alumimum-Lithium Alloys.* Eds. M. Peters and P. J. Winkler. DGM, Oberrursel, pp. 1165–1170.

3. Sunwoo, A. J., Bradley III, E. L., and Morris, J. W. 1990. *Metallurgical Transactions* 21A: 2795–2804.

4. Biermann, B., Dierken, R., Kupfer, R., Lang, A., and Bergmann, H. W. 1992. *Alumimum-Lithium Alloys.* Eds. M. Peters and P. J. Winkler. DGM, Oberrursel, pp. 1159–1164.

5. Zacharia, T., David, S. A., Vitek, J. M., and Martukanitz, R. P. 1989. *Aluminum Lithium Alloys: Proc. of 5th. Intl. Al-Li Conf.* Eds. T. H. Sanders, Jr., and E. A. Starke, Jr. Birmingham, U.K., MCE Pub., pp. 1387–1396.

6. Fridlyander, I. N., Dritz, A. M. and Krymova, T. V. 1992. *Alumimum-Lithium Alloys.* Eds. M. Peters and P. J. Winkler. DGM, Oberrursel, pp. 1245–1250.

7. Martukanitz, R. P., Natalie, C. A., and Knoefel, J. O. 1987. *Journal of Metals* 39: 38–42.

8. Myhr, O. R., and Grong, O. 1991. *Acta Metall. Mater.* 39(11): 2693–2702.

9. Easterling, K. E. 1992. *Introduction to the Physical Metallurgy of Welding,* Oxford, U.K., Butterworth-Heinemann.

10. Ion, J. C., Easterling, K. E., and Ashby, M. F. 1984. *Acta Metall.* 32(11): 1949–1962.

11. Ashby, M. F., and Easterling, K. E. 1982. *Acta Metall.* 30: 1969–1978.

12. Huang, J. C., and Ardell, A. J. 1989. 4th Intl. Aluminum-Lithium Conf. Eds. G. Champier *et al., Journal de Physique* 48, Colloque C3, pp. 373–383.

13. Pickens, J. R., Heubaum, F. H., Langan, T. J., and Kramer, L. S. 1989. *Aluminum Lithium Alloys: Proc. of 5th. Intl. Al-Li Conf.* Eds. T. H. Sanders, Jr., and E. A. Starke, Jr. Birmingham, U.K., MCE Pub., pp. 1397–1414.

14. Gayle, F. W., and Hewbaum, F. H. 1990. *Scripta Metall. Mater.* 24: 79–84.

15. Huang, J. C., and Ardell, A. J. *Acta Metall.* 36(11): 2995–3009.